Proceedings of the International Conference on Nanotechnology: Fundamentals and Applications
Ottawa, Ontario, Canada, 4-6 August 2010
Paper No. 478

An Investigation on the Milling and Hydrogen Reduction Behavior of Nanostructured W-Cu Oxide Powder

Eltefat Ahmadi [a, b], Mahdieh Malekzadeh [a, b], S.Khatiboleslam Sadrnezhaad [b, c]
[a] Research and Engineering Company for Non-ferrous Metals (RECo), Zanjan, Iran.
[b] Materials and Energy Research Center, Karaj, Iran
[c] Sharif University of Technology, Department of Materials Science and Engineering
Tehran, Iran
elt_ahmadi@yahoo.com; m_malekzadeh@mehr.sharif.ir; sadrnezh@sharif.edu

ABSTRACT

A two-step spex ball milling/hydrogen reduction was used to synthesize W-15 wt%Cu nanocomposite powders. WO_3 and CuO nano-powders were ball-milled under air/stearic acid for 1, 2 and 3 h. Then hydrogen-reduction was carried out at 650, 700 and 750°C for 15–90 min and sintering was performed at 1200°C for 60 min. Morphology and grain size of the products were rigorously investigated by scanning electron microscopy (SEM), transmission electron microscopy (TEM), X-ray diffraction (XRD) and nano-particle Zeta-sizer. The mean grain size of the homogenous powders milled under stearic acid for 3h was ~63 nm. Hydrogen reduction at 700°C for 90 min showed an average particle and cluster size of 60 and 445 nm, respectively. The mixture had a homogeneous structure with 16.1 ± 0.1 g/cm3 density when sintered at 1200 °C for 60 min.

1 INTRODUCTION

Nanocomposite tungsten alloys such as W-Cu, W-Ni-Cu, W-Fe-Ni and W-Co-Mn have received considerable attention, recently as shown by Ahmadi et al. (2010), Akhtar et al. (2008), Kim et al. (2005), Kim et al. (2004a,b), Wang et al. (1998), Yoon et al. (2002). Owing to their excellent conductivity, high wear resistance and thermal managing power, W–Cu composites are applicable in ultrahigh-voltage electric contactors, microelectronic devices, microwave blocking packages and high density integrated circuit heat sinks as shown by Dorfman et al. (2002), Lee et al. (2002). Conductivity of the heat-sink material is a significant parameter affected by homogeneity and compactness of the W–Cu composite article. Achieving full density by sintering of W and Cu powders is, therefore, extremely difficult. Because of large differences between their densities (19.3 g/cm3 for W and 8.9 g/cm3 for Cu), their homogeneous mixing is also laborious. Literature survey shows that mechanochemical processes (MCP) consisting of ball-milling and hydrogen reduction of WO_3-CuO mixtures can be used for processing of W-Cu nanocomposite powders as shown by Kim et al. (2004a, b), Lee et al. (2002). A desirable way of property improvement without addition of activating agent is to increase sintering capability by dramatic decreasing of the particle sizes of W–Cu composite articles as shown by Ahmadi et al. (2010), Dorfman et al. (2002).

The reduction paths are schematically illustrated in Figure 1 as shown by Schubert (1990). According to the Figure 1, hydrogen-reduction can occur via different routes. One route consists for example of: (a) WO_3 conversion into $WO_{2.9}$ and (b) reduction of $WO_{2.9}$ first into β-W and then into α-W. The temperature required for reduction of CuO is about 400°C. WO_3 converts to

$WO_{2.9}$ at about 380°C; while $WO_{2.9}$ reduces to W above 775°C as shown by Haubner et al. (1983a, b). To the best of our knowledge no details are available on the effect of process variables on spex ball milling/hydrogen reduction of nanostructure W–Cu oxide powders.

In this study, the effect of the spex ball-milling under stearic acid on the morphology and size of WO_3- CuO powders, hydrogen reduction parameters (i.e. time and temperature) and also the final morphology of W-Cu composite reduced/sintered powders were considered using TEM, SEM, nano-particle Zeta-sizer and XRD methods. The results indicated that when the initial oxide mixture was nano-structured via spex ball milling, the nanocomposite product densified close to the theoretical density (16.5 g/cm^3) and its grains became superior. No additives (Co, Ni, Pd, etc.) were needed to obtain the required densification in this case.

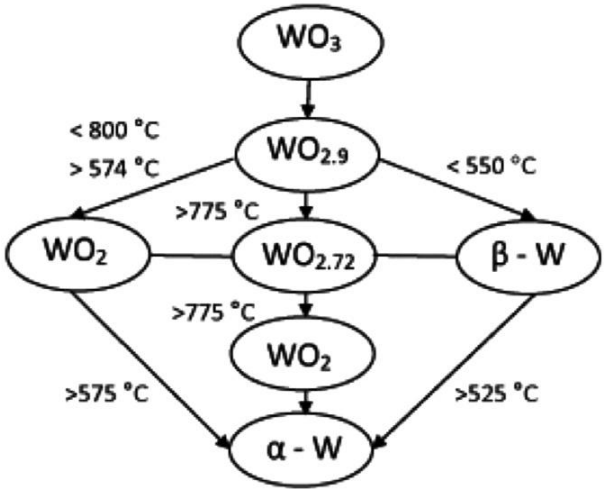

Figure 1: Schematic flowchart of yellow tungsten oxide (YTO: WO_3) reduction

2 EXPERIMENTAL PROCEDURE

tungsten oxide powder (WO_3) with mean particle size of 13 microns and purity of 99.97% (Wolfram Company JSC, Russia) and copper oxide (CuO) powder with mean particle size of 1.5 microns and purity of 99.9% (Merck, Germany) were ball-milled in 8000 Spex mixer/miller under stearic acid for 1, 2 and 3 h. Ball-milling was carried out in a stainless steel cup containing stainless steel balls. The ball-to-powder weight ratio was 8:1. The stainless steel balls had 5mm diameter. The tungsten-copper powders were initially spex ball-milled under air/stearic acid atmosphere and were isothermally reduced by a flow of about 0.2 l/min gaseous hydrogen (99.9995%) of having pressure dew point of -70 °C (Hydrogen Generator PH300, UK) at 400, 650, 700 and 750°C for 15–90 min. The first reduction step took 30 min at 400 °C. The second step timed 15, 30, 45, 60, 75 and 90 min at 650, 700 and 750 °C. The boats containing the mixture were made of recrystallized alumina. The boatload weighed ~1.5 g with a height of ~2 mm. The morphology and particle size of the nano-composite powders were obtained by scanning electron microscope (SEM, VEGA, TESCAN Czech Republic), transmission electron microscopy (TEM, ZEISS-EM 900, West German), X-ray diffraction (XRD, Powder Metallurgy 9920/50, Philips, Holland) with Cu Ka radiation having 0.15405 nm wavelength and Zeta potential and size analyzer (Zeta-sizer 3000 HS) at the room temperature. An argon-quench was accomplished at the end of each step in order to assess the reduction behavior of the specimens. Eventually, nano-structured mixtures were compacted under 300 MPa pressure, then were heated-up at a heating rate of 10 °C/min up to 1200°C under hydrogen and sintered at 1200 °C for 60 min. Microstructure of the sintered specimen was characterized by SEM.

3 RESULT AND DISCUSSION

3.1 The effect of spex ball milling on morphology and size of WO_3- CuO powders:

Figure 2 shows the XRD pattern of the WO_3–CuO powder mixtures ball-milled by Spex mixer-miller under stearic acid in a stainless steel cup with stainless steel balls for 1, 2 and 3 hours. The XRD patterns given in Figure 2 indicate that by increasing the ball-milling time, the peaks for WO_3 and CuO phases broaden and become distinguished. After 3h, CuO peaks nearly disappear due to the refinement of the grains. The grain sizes of the WO_3 and CuO in wet-milling under stearic acid are significantly decreased by increasing the milling time. The peak of $CuWO_4$ indicated in the XRD patterns (Figure 2) shows that $CuWO_4$ forms by milling for any time. Formation of $CuWO_4$ by mechanical milling has been reported by other researchers, too as shown by Yoon et al. (2002), Li et al. (2003). For long milling time, inter-diffusion of oxides leads to $CuWO_4$ spinel phase formation.

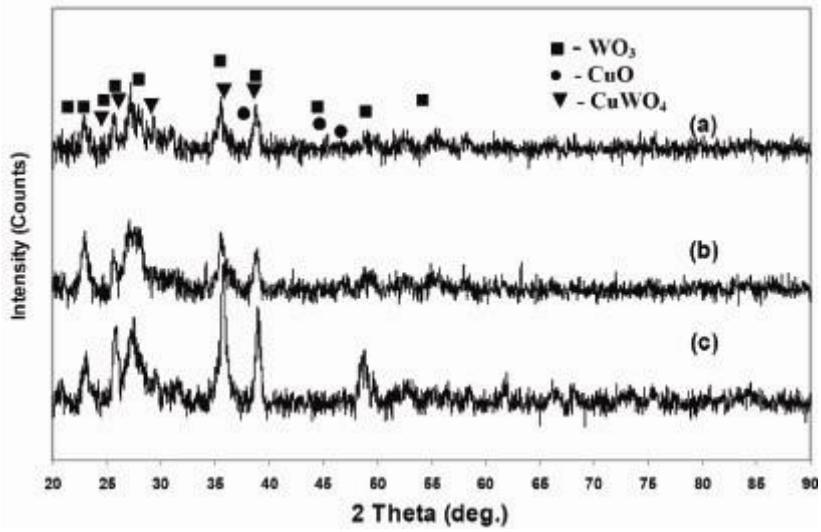

Figure 2: The XRD patterns of the ball milled WO_3-CuO powders under stearic acid in stainless steel cups with stainless steel balls for (a) 3h, (b) 2h and (c) 1h.

Scanning electron microscopy (SEM) was employed for further investigation of the microstructure of the spex ball-milled powder mixtures for different times under air/stearic acid. Morphologies of both ball milled powders are compared in Figures 3(a) and (b). Results show that the morphology of the powders milled under stearic acid in stainless steel cup and balls is more homogeneous than the samples dry-milled under air. Hence, milling under stearic acid for 3h in Spex mixer–miller is more desirable for production of WO_3-CuO nano-structured powder mixture. The mean particle size of the ball-milled powders under stearic acid for 3h is about 63nm as shown in Figure 3(b).

It can be inferred from Figure 3(a) that the powders laminated and largely aggregated by small WO_3 aggregate particles contacting CuO. Comparing the results of the dry-milling (Figure

3(a) and (b)) with the wet-milling indicate that the wet milling under stearic acid is much better than the dry one. Under stearic acid as a PCA in stainless steel cup, the fracture mechanism overcomes rigorously to the cold welding during wet-milling. The Zeta-sizer results are plotted in Figure 4 showing two peaks related to the (a) agglomerates and (b) the smaller embedded grains. The average size of the latter was about 65 nm. Therefore, the Zeta-sizer results confirm SEM results.

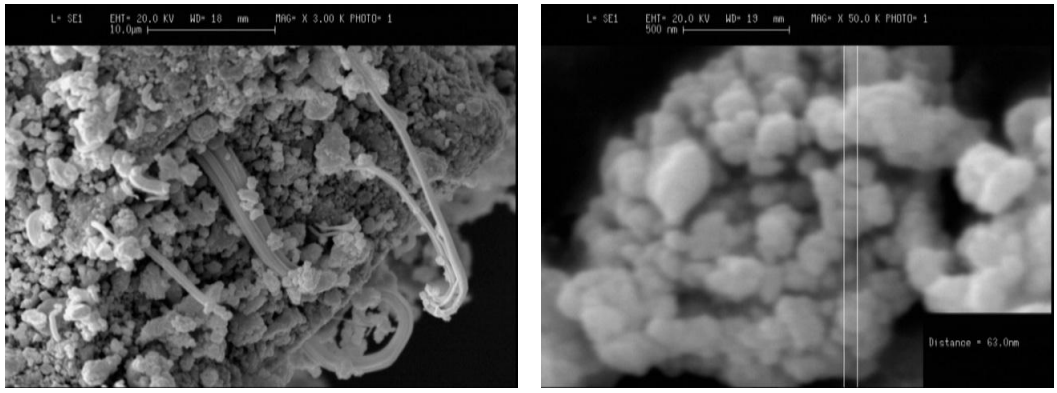

(a) (b)

Figure 3: SEM morphology of WO_3-CuO powder mixture ball milled under (a) air and (b) stearic acid in stainless cup containing stainless steel balls for 3h.

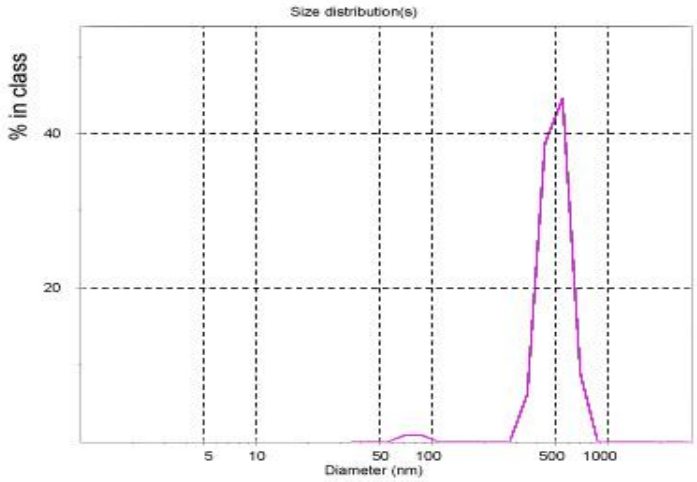

Figure 4: The Zeta-sizer result of WO_3-CuO powder mixture ball milled under stearic acid for 3h.

3.2 The influence of time and temperature on hydrogen reduction process:

Figure 5 shows the diffraction patterns obtained from the XRD analysis of the W–Cu nanocomposite powder after reduction with hydrogen at three different temperatures: 650, 700 and 750°C for 15, 30, 45, 60, 75 and 90 min. The peaks observed in Figure 5(a) belong to WO_3, $WO_{2.9}$, $WO_{2.72}$, WO_2 and Cu. No primal changes occurred with the time in the samples. Figure 5(b) illustrates the XRD patterns of the powders partially reduced at 700°C. The existence of all intermediate and final phases of WO_3, $WO_{2.9}$, $WO_{2.72}$, WO_2 and the elemental copper were clearly assessable at all times. Figure 5(c)

shows the XRD patterns of W–Cu nano-composite powders produced by full reduction of WO_3–CuO mixture for different times at 750 °C. At longer reduction times (i.e. 90 min), the peaks corresponding to W and Cu especially became noticeable. The $WO_{2.9}$, $WO_{2.72}$ and elemental Cu phases were also formed at the first reduction step taking place at 400°C.

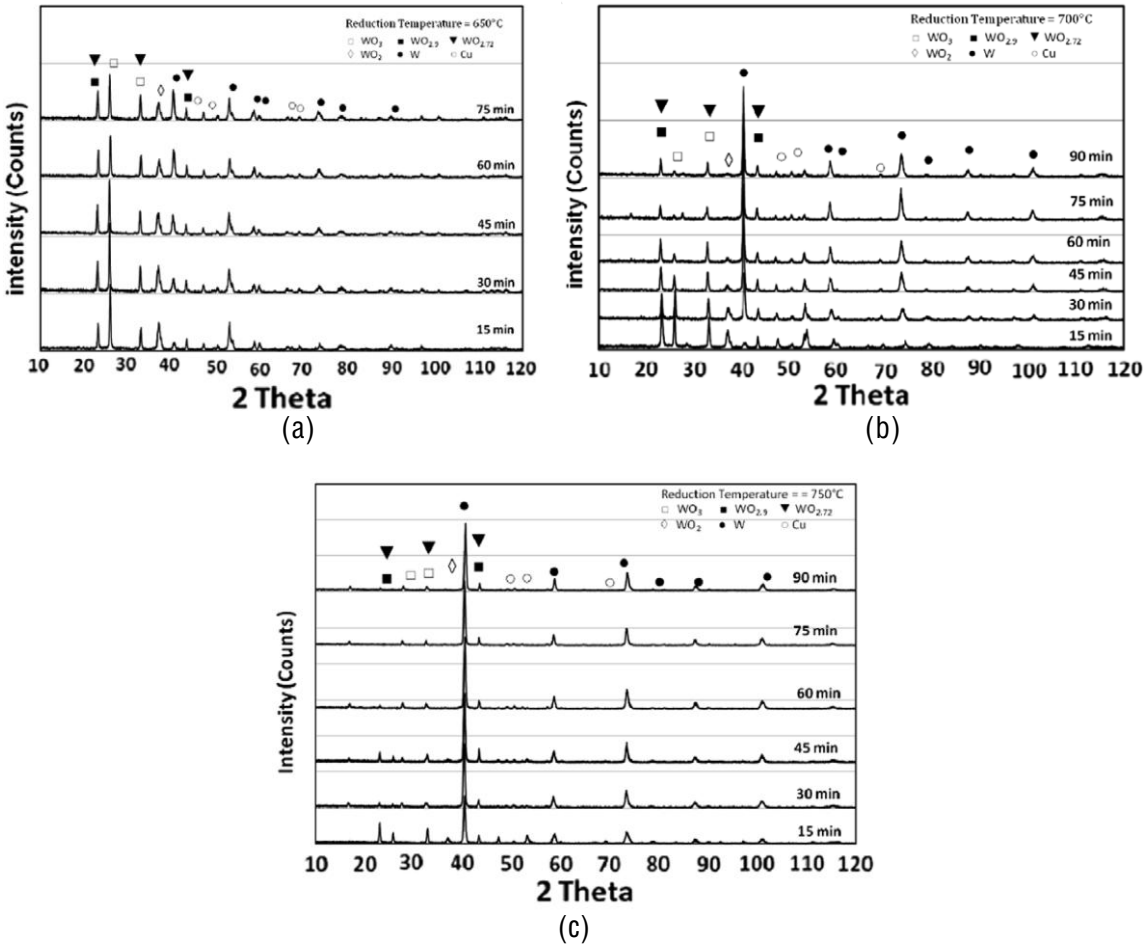

Figure 5: XRD patterns of nanostructured W–Cu powders produced by hydrogen-reduction of WO_3–CuO at: (a) 650°C, (b) 700°C and (c) 750°C for different times.

Formation of the intermediate $WO_{2.72}$ and WO_2 phases during the hydrogen reduction was one of the most remarkable differences between 650°C and 700°C as shown in Figures 5(a) and 5(b). Reduction of WO_3–CuO mixture into metallic W–Cu nano-composite powder could, thus, be divided into the following three main reduction steps:

$$WO_3—CuO \rightarrow WO_{2.9}—WO_{2.72}—Cu \rightarrow WO_2—Cu \rightarrow W—Cu \qquad (1)$$

Figure 6 shows the SEM images of the nano-structured W–Cu powder mixtures produced at different temperatures for 90 min. As is seen, morphological changes accompanied with cluster size enhancement occur with increasing of the reduction temperature. Significant changes in the SEM morphology were observed in Figure 6. More clusters form at 750°C as compared to the other reduction temperatures and nanoparticles obtained at 700°C were much smaller than those of at 750°C (Figure 6). This is due to the faster reduction of WO_3– CuO mixture at higher temperatures (e.g. 750°C). From Figure 6(b) and(c), the sizes of the clusters are determined to be about 445 nm and the mean particle size

of W nanopowder reduced at 700 and 750°C for 60 min and above is about 70 nm (always less than 200 nm) with a homogeneously mixed structure obtained by wall to wall tool of a SEM.

Hydrogen reduction ended with agglomerated clusters with average diameter of 445 nm (according to SEM) and 492 nm (according to the Zeta-sizer) embedding reduced grains of ~70 nm mean dimension (Figures 6(b) and 7). The Zeta-sizer results plotted in Figure 7 showing two peaks related to the (a) clusters and (b) the smaller embedded grains. The average size of the latter was about 95 nm.

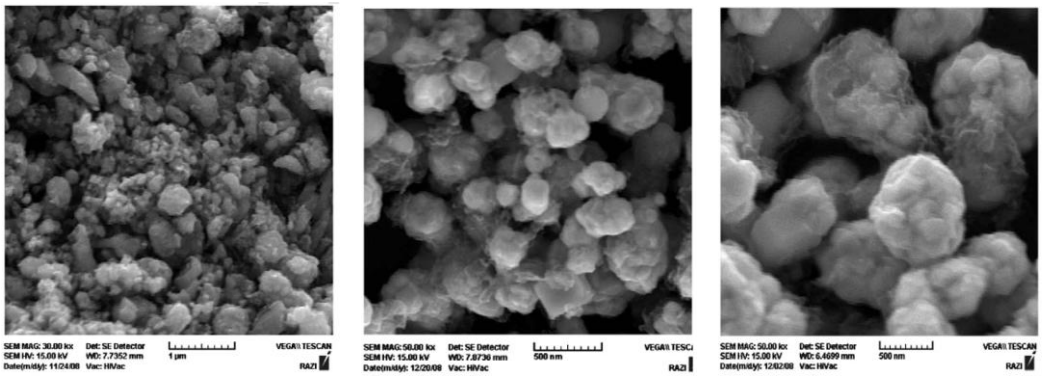

(a) (b) (c)

Figure 6: SEM morphology of W–Cu powders produced by hydrogen reduction of milled WO_3–CuO mixture for 90 min at: (a) 650, (b) 700 and (c) 750°C.

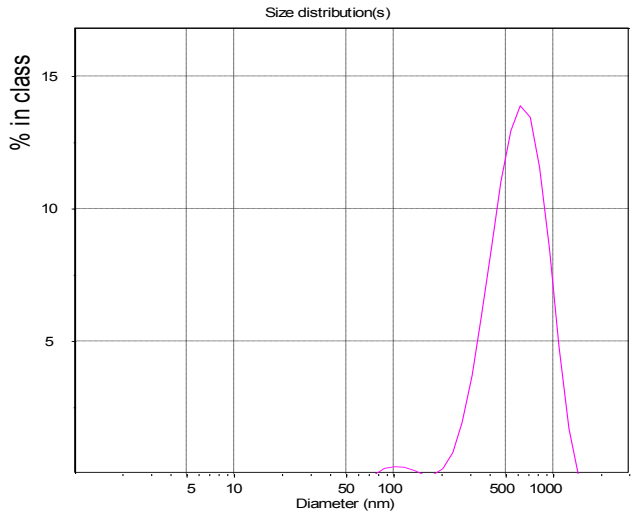

Figure: 7 Zeta-sizer results indicating average grain size of both the embedded and the agglomerated grains produced after hydrogen reduction at 750°C.

The typical TEM image of W-Cu nanopowder reduced under gaseous hydrogen at 700°C for 90min is given in Figure 8. As is seen, a number of small particles of about 60 nm in diameter obtained by hydrogen reduction.

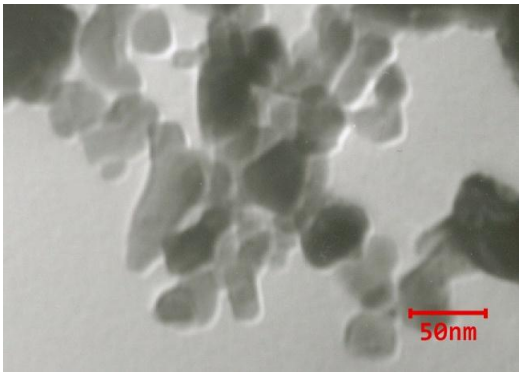

Figure 8: TEM image of the nanostructured W-Cu powder hydrogen-reduced at 700°C for 90 min.

Based on the previous investigations, hydrogen-reduction of tungsten oxides is controlled by solid-state diffusion (oxygen transport) or chemical vapor transport (CVT) of tungsten atoms as shown by Schubert et al. (1990). It is, therefore, concluded that the first step of WO_3–CuO nano-powder reduction is $CuO \rightarrow Cu + 1/2O_2$ which takes place at ~400°C and at temperatures around 700°C, WO_3 reduces to α-W. The two-step reduction temperatures for production of W–Cu nanocomposite powder were consequently may be determined to be equal to 400 and 700°C, respectively.

SEM image of sintered specimen exhibited in Figure 9. The compact mixture sintered at 1200°C for 60 min has a homogeneous structure and density of 16.1 ± 0.1 g/cm^3 close to the theoretical density (TD) of the tungsten–copper composites composed of 85wt% tungsten and 15wt% copper (16.5 g/cm^3). It is clear that SEM morphology of the sintered W–Cu nanocomposite at 1200°C indicates sufficiently interconnected particles. This is due to the liquid phase sintering (LPS) of nanostructured W-Cu powders.

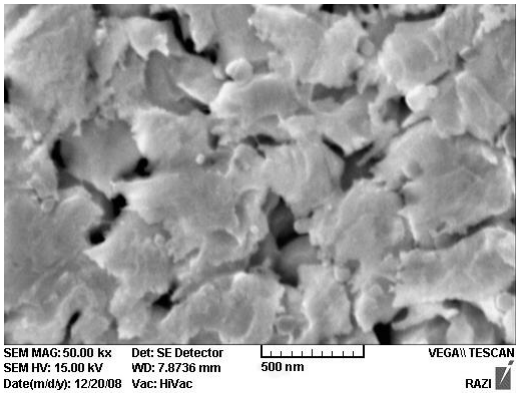

Figure 9: SEM image of the W–Cu nanocomposite hydrogen-reduced at 750°C and sintered at 1200°C for 60 min.

4 CONCLUSIONS

In this work, we studied the influence of milling time and hydrogen reduction parameters (time and temperature) on production of W-15%wtCuO nanocomposite. Results showed that milling under stearic acid for 3h in spex mixer–miller is appropriate for production of WO_3-CuO nanostructure powder mixtures. The morphology of the powders milled under stearic acid for 3h was desirably homogeneous with the mean grain size of ~63 and 65 nm estimated by SEM and Zeta-sizer results, respectively. SEM morphologies showed that specimens reduced at 750°C had more nano-particle clusters than those reduced at lower temperatures. The hydrogen-reduced aggregates at 700°C showed an average size of about 60 nm according to the TEM results. Production of the totally reduced W–Cu particulates was more feasible at 750°C. Intermediate transformation steps occurred at alternative reduction temperatures. At the

first reduction step, CuO reduced to Cu according to the reaction: $CuO \rightarrow Cu + 1/2O_2$, which took place at about 400°C. Reduction of WO_3 to α-W simultaneously may be occurred at ~700°C. The sintered specimens showed homogeneous W–Cu nanocomposite structure obtained by sintering at 1200°C.

5 ACKNOWLEDGEMENTS

The authors would like to thank the Materials and Energy Research Center (MERC) for its supports.

REFERENCES

Ahmadi E., Malekzadeh M. and Sadrnezhaad S.K. (2010). W–15 wt%Cu Nanocomposite Produced by Hydrogen-Reduction/Sintering of WO_3–CuO Nano-powder. Int. J. Refractory Metals & Hard Materials, 28, 441-445.

Akhtar F. (2008). An Investigation on the Solid State Sintering of Mechanically Alloyed Nano-structured 90W–Ni–Fe Tungsten Heavy Alloy. Int. J. Refractory Metals & Hard Materials, 26, 145–151.

Dorfman L.P., Houck D.L., Scheithauer M.J. and Frisk T.A. (2002). Synthesis and Hydrogen Reduction of Tungsten–Copper Composite Oxides. J. Materials Research, 17, 821–830.

Haubner R., Schubert W.D., Lassner E., Schreiner M. and Lux B. (1983). Mechanism of Technical Reduction of Tungsten, part I. Int. J. Refractory Metals & Hard Materials, 2, 108–115.

Haubner R., Schubert W.D., Hellmer H., Lassner E. and Lux B. (1983). Mechanism of Technical Reduction of Tungsten: part 2, Hydrogen Reduction of Tungsten Blue Oxide to Tungsten Powder. Int. J. Refractory Metals & Hard Materials, 2, 156–163.

Kim D.G., Kim G.S., Oh S.T. and Kim Y.D. (2004). The Initial Stage of Sintering for the W–Cu Nanocomposite Powder Prepared from W–CuO Mixture. Materials Letters, 58, 578–581.

Kim D.G., Lee K.W., Oh S.T. and Kim Y.D. (2004). Preparation of W–Cu Nanocomposite Powder by Hydrogen-Reduction of Ball Milled W and CuO Powder Mixture. Materials Letters, 58, 1199–1203.

Kim D.G., Lee B.H., Oh S.T., Kim Y.D. and Kang S.G. (2005). Mechanochemical Process for W–15wt.%Cu Nanocomposite Powders with WO_3–CuO Powder Mixture and its Sintering Characteristics. Materials Science and Engineering A, 395, 333–337.

Lee S., Hong M.H., Noh J.W. and Baek W.H. (2002). Microstructural Evolution of a Shaped- Charge Liner and Target Materials During Ballistic Tests. Metallurgical Materials Transaction A, 33, 1069–1074.

Li Y., Qu X., Zheng Z., Lei C., Zou Z. and Yu S. (2003). Properties of W-Cu Composite Powder Produced by a Thermo-Mechanical Method. Int. J. Refractory Metals & Hard Materials, 21, 259-264.

Schubert W.D. (1990). Kinetics of the Hydrogen Reduction of Tungsten Oxides. Int. J. Refractory Metals & Hard Materials, 9, 178–191.

Wang W.S. and Hwang K.S. (1998). The Effect of Tungsten Particle Size on the Processing and Properties of Infiltrated W–Cu Compacts. Metallurgical Materials Transaction A, 29, 1509–1516.

Yoon E.S., Lee J.S., Oh S.T. and Kim B.K. (2002). Microstructure and Sintering Behavior of W–Cu Nanocomposite Powder Produced by Thermo-Chemical Process. Int. J. Refractory Metals & Hard Materials, 20, 201–206.